

REPRESSION OF RETROTRANSPOSAL ELEMENTS IN MOUSE EMBRYONIC STEM CELLS IS PRIMARILY MEDIATED BY DNA METHYLATION-INDEPENDENT MECHANISM

Leah K Hutnick^{1,2}, Xinhua Huang¹, Tao-Chuan Loo¹, Zhicheng Ma¹ and Guoping Fan¹

¹Department of Human Genetics, ²Neuroscience Interdepartmental Program, David Geffen School of Medicine, UCLA, Los Angeles, CA 90095

Running head: Retrotransposon IAP regulation in mESCs and EpiSCs

Address correspondence to: Guoping Fan, Ph.D. Department of Human Genetics, David Geffen School of Medicine, UCLA, 695 Charles Young Drive South, Los Angeles, CA 90095 USA. Phone: (310) 267-0439; Fax: (310) 794-5446; Email: gfan@mednet.ucla.edu

In defense of deleterious retrotransposition of intracisternal A-Particles (IAP) elements, IAP loci are heavily methylated and silenced in mouse somatic cells (1). To determine whether IAP is also repressed in pluripotent stem cells by DNA methylation, we examined IAP expression in demethylated mouse embryonic stem cells (mESCs) and epiblast-derived stem cells (EpiSCs). Surprisingly, in demethylated ESC cultures carrying mutations of DNA methyltransferase I (Dnmt1), no IAP transcripts and proteins are detectable in undifferentiated Oct4⁺ ESCs. In contrast, approximately 3.6% of IAP positive cells are detected in Oct4⁺ Dnmt1^{-/-} cells, suggesting that the previously observed increase in IAP transcripts in the population of Dnmt1^{-/-} ESCs could be accounted for by this subset of Oct4⁺ Dnmt1^{-/-} ESCs undergoing spontaneous differentiation. Consistent with this possibility, a dramatic increase of IAP mRNA (>100 fold) and protein expression was observed in Dnmt1^{-/-} ESC cultures upon induction of differentiation through the withdrawal of leukemia inhibitory factor (LIF) for six or more days. Interestingly, both mRNAs and proteins of IAP can be readily detected in demethylated Oct4⁺ EpiSCs as well as differentiated MEFs, neurons and glia upon conditional *Dnmt1* gene deletion. These data suggest that mESCs are a unique stem cell type possessing a DNA methylation-independent IAP repression mechanism. This methylation-independent mechanism does not involve Dicer-mediated action of microRNAs or RNA interference because IAP expression remains repressed in Dnmt1^{-/-}; Dicer^{-/-} double mutant ESCs. We suggest that mESCs possess a unique DNA methylation-independent mechanism to silence

retrotransposons to safeguard genome stability while undergoing rapid cell proliferation for self-renewal.

DNA methylation, an epigenetic modification where a methyl group is covalently added to the cytosine of CpG dinucleotides, is catalyzed by a family of DNA methyltransferases (Dnmts) that include *de novo* (Dnmt 3a, 3b) and maintenance methyltransferases (Dnmt1) (2-3). DNA methylation is known to regulate developmental gene expression, genomic imprinting, X-inactivation, and genomic stability (4-9). Many retrotransposable repetitive elements are heavily methylated (10), and current evidence supports a causal relationship between DNA methylation and repression of retrotransposons(11). Intracisternal A particles (IAPs) are murine endogenous retroviral repetitive elements, with an estimation of over 1000 copies across the haploid murine genome (12-14). Germ line mutations due to IAP retrotransposition most often occur at intronic sites, disrupting gene expression through premature termination, aberrant splicing, or viral LTR-driven transcription (15). Furthermore, insertional mutagenesis of IAP elements is noted in various murine cancer cell lines with subsequent activation of oncogenes or cytokine genes (16-17).

When expressed, IAP proteins are non-infectious viral particles that are retained in the cisternae of the endoplasmic reticulum (18). IAP proteins can be transiently detected in pre-implantation embryos, when DNA methylation is temporarily decreased (1,19). In established lines of mouse embryonic stem cells (ESCs) derived from the inner cell mass, IAP elements are already heavily methylated with little detectable IAP expression (20).

In this article, we examined expression of IAP proteins in control and demethylated somatic cells, EpiSCs, and mESCs. Using a previously generated antibody against IAP protein (p73) (21) as well as our polyclonal antibody raised against recombinant IAP *gag* protein (11,22), we mapped changes in IAP protein levels after *Dnmt1* gene deletion in floxed (*Dnmt1*^{2lox/2lox}) mouse embryonic fibroblasts (MEFs) using viral-mediated cre-recombinase. Unexpectedly, we found IAP mRNA and protein levels are not detected in Oct4⁺ *Dnmt1*^{-/-} ESCs, but are dramatically increased in demethylated mESC cultures upon *in vitro* differentiation, suggestive of the presence of DNA methylation-independent repression mechanism(s) in silencing IAP expression in undifferentiated mESCs.

Experimental Procedures

Antigen generation and anti-IAP2 purification- Sequence from plasmid M1A14 (22) was used to clone the IAP2 fragment (250-750aa) into pGEX4T3 vector (Fig. 1) (11). After IPTG induction, bacteria were harvested and the IAP2-GST fusion protein was purified with glutathione beads (Amersham Pharmacia). After evaluation of the thrombin-cut eluate, antigen was shipped to PickCell Laboratories for rabbit immuno-injection. Rabbit polyclonal serum was tested and evaluated before purification. Briefly, GST-IAP2 fusion protein was adsorbed onto glutathione beads (Roche Diagnostics protocol), fixed by 20 mM DMP (dimethyl pimelimidate) in 200 mM pH 8.5 HEPES buffer, and terminated in 200 mM pH 8.3 Tris-HCl buffer. Antibody bound to IAP2-GST fusion protein was washed with TBS and eluted by 200 mM glycine (pH 2) followed by neutralization with 1 M pH 8.5 Tris-HCl buffer to pH 7.4. Eluates were examined by immunoblotting at different dilutions in three independent trials to verify specificity.

Viral production and infection- MSCV-cre-gfp and MSCV-gfp were generated in HEK 293T cells via calcium phosphate transfection. For viral infection, cells were trypsinized and resuspended in 1 mL of cell media (90% DMEM, 10% FBS, 1x Penicillin/Streptomycin, 1 mM glutamine) with polybrene (8 µg/ml). Cells in suspension were incubated with titered virus. After 30 minutes, the infected cells were added to gelatinized wells and coverslips. Media was changed after 6-8 hours. During the time course, corresponding wells were

harvested for DNA, RNA, and protein. Coverslips were retrieved and fixed in 4% paraformaldehyde for 15 minutes at room temperature for immunocytochemistry.

Lentivirus (LV-cre-gfp) was generated by the UCLA Department of Medicine VectorCore with a concentration of 1.6×10^7 pfu/ml. Cre recombinase activity was verified by infecting fibroblasts generated from *R26R βgeo* line (23). To infect mESCs, cells were grown feeder free for 2 passages, and after trypsinization, 5×10^5 cells were resuspended in 1 ml of LV-cre supernatant plus 8 µg/ml polybrene and rotated in eppendorf tubes for 2 hours at 37°C. Cells were pelleted, washed twice with media, and plated low density onto feeders with coverslips to monitor acute infection. For subcloning analysis, infected single cells were enriched using flow cytometry sorting (FACsVantage, UCLA JCCC Flow Cytometry Core), plated at low density, and individual colonies picked and expanded for DNA, RNA, and immunohistochemistry.

Epiblast stem cell derivation and culture- *Dnmt1*^{2lox/2lox} mice were mated and at E5.5, post-implantation embryos were dissected and cultured as described with minor modifications to the protocol (35). EpiSC cultures were maintained on gamma-irradiated feeders in EpiSC media (DMEM/F12 supplemented with 7 µg/ml insulin, 15 µg/ml transferrin, 5mg/ml BSA, 12 ng/ml FGF-2, 20 ng/ml activin-A, 1000 units/ml LIF, 1x Penicillin/Streptomycin, and 450 µM monothiolglycerol). EpiSCs were passaged using collagenase dispase dissociation into small colonies. For lentiviral infection, EpiSCs were dissociated in 0.25% Trypsin-EDTA, preplated to remove feeders, and infected using the above described procedure.

Mouse ES cell culture- Wild-type control (J1 cells), *Dnmt1*^{-/-} (c/c ESCs) (24), *Dnmt1*(kd), *3a*^{-/-}, *3b*^{-/-} [TKO cells (25), a kind gift from Dr. Rudolf Jaenisch, Whitehead Institute] and *Eed*^{-/-} mESCs (generously provided by Dr. Terry Magnuson, UNC) were cultured under standard conditions on DR4 gamma-irradiated feeders, changing media daily (85% high glucose DMEM, 15% ES screened FBS (Hyclone), 1 mM Glutamine, 1x Penicillin/Streptomycin, 0.1 mM non-essential amino acid, 0.1 mM β-mercaptoethanol, 500 units LIF/ml) and passaging

using Trypsin-EDTA. For partial differentiation, mouse ES cells were plated 0.2% gelatin B coated plates and coverslips. After 24 hours (Day 0 time point), media was changed to LIF⁻ differentiation media (90% DMEM, 10% FBS, 1x Penicillin/Streptomycin, 1 mM glutamine). Media was changed every day, with corresponding wells harvested for DNA, RNA, protein, and coverslips over the time course (Day 0-Day 12).

Immunoblotting- Immunoblotting procedure was performed as previously described (26). The original IAP antibody (anti-p73, clone 37.11X from Dr. Kira Lueders) was used at a dilution of 1:1000 and incubated overnight at room temperature. Our IAP2 antibody was used at a 1:2000 dilution for western blots. Anti-GAPDH (Abcam, 1:5000) was used as loading control.

RNA purification and qRT-PCR- Total RNA was harvested by TRIzol as per manufacturer's instructions (Invitrogen). RNA was converted to cDNA using iScript reaction Kit (Bio-Rad). qRT-PCR was performed using Bio-Rad MyCycler and Sybergreen Supermix (Biorad). Results were normalized to 18s values expressed as fold change relative to corresponding control values (27). P values were assessed using Student t-test (2-tailed, paired).

IAP F AAG CCC TTT TGT TCC TTT TCA
IAP R ACC CTT GGA AAG GCC TGT AT
18s F GCC CTG TAA TTG GAA TGA GTC
CAC TT
18s R CTC CCC AAG ATC CAA CTA CGA
GCT TT

IAP2 Fluorescent in situ hybridization (FISH) and Northern Analysis- IAP2 (250aa-700aa) sequence was PCR amplified from the MIA14 plasmid gel purified (Promega). 100 ng of IAP2 template was used to generate a Cy3 labeled cDNA probe using the Bioprime Kit (Roche Applied Sciences) as per manufacturer's instructions. FISH was carried out as previously described (28). The same amplified region was used to create a Northern probe. Northern blot analysis was performed using the standard procedure in our previous publication (26). **Immunostaining-** Coverslips were picked and fixed in 4% paraformaldehyde for 15 min and washed 3 times (5 min each) with 1xPBS. Blocking and permeabilization were carried out for 1 hour with 0.5% Triton X-100 in PBS plus 10% normal goat serum. Primary antibody diluted in PBS plus 1% normal goat serum and 0.1%

Triton X-100 was added to coverslips and incubated overnight at room temperature. Primary antibodies used were the following: anti-IAP2 (rabbit polyclonal, 1:1000), anti-Oct 3/4 (Santa Cruz Biotechnology, mouse monoclonal, 1:20). Anti-H4K20 3me (Millipore, mouse monoclonal, 1:500) was incubated at room temperature for 1 hour. Coverslips were washed and secondary antibody (Jackson ImmunoResearch) diluted in PBS plus 1% normal goat serum and 0.1% Triton X-100 was added for 1 hour.

Section immunohistochemistry was performed as previously described (29). The original anti-IAP (p73) antibody was diluted (1:500) in PBS containing 5% normal goat sera, 3% BSA, and 0.25% TritonX overnight at room temperature. Our IAP2 antibody was used at 1:1000 in PBS plus 5% normal goat serum and 0.25% Triton X. The next day, the sections were washed in 1XPBS 3x 10 minutes, and then secondary antibody (Jackson ImmunoResearch) was applied for 2 hours at room temperature.

Confocal fluorescence- Images were taken at 63X magnification using Leica Confocal Software on a Leica TCS-SP MP Confocal and Multiphoton Inverted Microscope (Heidelberg, Germany) equipped with an argon laser (488 nm blue excitation: JDS Uniphase), a 561 nm (green) diode laser (DPSS: Melles Griot), a 633 nm (red) helium-neon laser and a two photon laser setup consisting of a Spectra-Physics Millennia X 532 nm green diode pump laser and a Tsunami Ti-Sapphire picosecond pulsed infrared laser tuned at 768 nm for UV excitation.

Results

IAP antiserum detects the gag protein encoded in IAP elements, which is expressed in demethylated fibroblast cells. Given that IAP repeats are heavily methylated by Dnmt1, we asked whether IAP protein could be detected in DNA demethylation models. The original p73 anti-sera also recognizes other proteins containing partial products of IAP coding regions (22) (Fig 1B). For specific recognition of IAP gag protein product, we created a recombinant protein fusing GST to a partial fragment of IAP gag protein (IAP2, 251-699 aa) (Fig 1A). Once purified over IAP2-GST columns, the original sera yielded a clean p73 band via immunoblot in tissue possessing over 95% *Dnmt1*^{-/-} cells in the central nervous system (29) (Fig 1B). The purified serum was partially blocked by

pre-adsorption against IAP2 peptide fragment, indicating the specificity of anti-serum (Fig 1B). We used this recombinant IAP2 protein fragment to generate a separate polyclonal antibody for both immunoblotting and immunostaining assays to detect IAP protein expression (Fig 1B).

To examine the onset of IAP protein reactivation after *Dnmt1* gene deletion, *Dnmt1*^{2lox/2lox} MEFs were infected with retrovirus containing cre-recombinase fused to green fluorescent protein (MSCV-cre-gfp) (30). Significant genomic demethylation was detected after 4 days post infection via southern blotting for the IAP repeat probe (Fig 2A). As DNA methylation levels drop after the deletion of *Dnmt1*, we found reactivation of IAP protein translation in infected cells starting 5 days post-infection via immunoblot (Fig 2B). When individual cells were examined for IAP immunoreactivity, IAP protein was detectable in a minority of infected cells as early as 4 days post-infection (Fig 2C). IAP expression was restricted to the cre-GFP infected cell population (arrows, Fig 2C). Thus the reactivation of IAP protein expression is tightly associated with onset of genomic DNA demethylation caused by the deletion of *Dnmt1*.

IAP protein immunostaining marks demethylated cells and cultured neuroblastoma cells at a single cell resolution. We next asked whether IAP protein could be used to detect demethylated cells at a single cell resolution in the developing nervous system after conditional *Dnmt1* deletion in neural precursors. Using our anti-IAP2, IAP immunoreactivity was restricted to the zone of *Dnmt1* deletion as dictated by the expression pattern of *Emx1-cre* and *Nestin-cre* (Fig. 3A and 3B) (11, 29). In the *Emx1-cre* driven deletion of *Dnmt1*, no immunoreactivity for IAP was seen in control regions of striatum, thalamus, brain stem, or cerebellum where DNA methylation is maintained (data not shown).

The neuroblastoma cell line N2a, which is known to transcribe certain IAP-LTR containing genes (31-32), shows strong anti-IAP2 immunoreactivity in the cytoplasm with a characteristic juxtanuclear staining pattern for viral A particles (Fig 3C). Endogenous IAP protein levels are strongly reactivated in N2a cultured cells, which correlates with the known hypomethylation of IAP elements in the N2a

genome (32). Thus, IAP immunoreactivity is a very useful tool to locate demethylated cells in a variety of DNA demethylation models.

Demethylated embryonic stem cells do not contain detectable IAP mRNAs and proteins yet exhibit dramatic IAP induction upon differentiation. *Dnmt1*^{-/-} mESCs possess less than 22% normal genomic methylation levels and exhibit increased expression of IAP mRNAs (24, 25). Surprisingly, when we performed Western blot analysis to assay IAP proteins, we could not detect IAP proteins in lysate from undifferentiated *Dnmt1*^{-/-} mESCs cultures (Fig 4A). When we used IAP fluorescent in situ hybridization (FISH) to detect mRNA signal in the undifferentiated *Dnmt1*^{-/-} mESCs, we did not visualize increased IAP mRNA levels (Figure 4E, Day 0). We then performed co-immunostaining of IAP and Oct3/4 to verify whether individual cells express IAP protein in the undifferentiated state. Only a small minority of IAP positive cells existed in *Dnmt1*^{-/-} cultures (3.6%±0.51%, mean±SE, n= 825 cells, Figure 4D Day 0), but all IAP positive cells were Oct3/4 negative, indicative of differentiation. IAP protein reactivation in this minor population may be below immunoblot detection levels, yet the level of IAP transcripts was elevated sufficiently in this differentiated subset to account for detection by more sensitive qRT-PCR assay in the population of *Dnmt1*^{-/-} ESCs.

We next examined the time course of IAP immunoreactivity in demethylated mESCs after in vitro differentiation. Upon LIF withdrawal in the absence of feeder cells, *Dnmt1*^{-/-} mESCs undergo a dramatic increase in IAP transcription and translation (Figure 4B, 4C). Quantitative RT-PCR reveals a 10-fold increase in IAP transcript levels 5 days after LIF withdrawal in *Dnmt1*^{-/-} cells. Moreover, a similar profile of mRNA expression is detected using FISH labeling and northern blot analysis specific for IAP2 (Figure 4E-F). After 6 days of LIF withdrawal IAP protein is detectable in total cell lysate (Day 6 long exposure, Figure 4C). By day 9 of the LIF withdrawal time course, we see robust protein expression (Figure 4C) and a corresponding 103± 29 fold relative increase of IAP transcription in *Dnmt1*^{-/-} cultures (p< 0.0001, Figure 4B). Z-stack confocal microscopy through individual colonies revealed IAP immunoreactivity present only in cells with low or no Oct3/4 immunoreactivity throughout the time

course (Figure 4D). Over the course of LIF withdrawal, the differentiated population increases dramatically (Figure 4D), and only after a significant increase in this population was the threshold for immunoblot detection reached.

Detection of IAP protein expression in demethylated epiblast-derived stem cells (EpiSCs)

To determine if DNA methylation-independent mechanism in suppression of IAP elements is unique to pluripotent stem cells such as mESC, we derived *Dnmt1*^{2lox/2lox} EpiSCs and examine the effect of DNA demethylation on IAP expression. EpiSCs are derived from the epiblast of the post-implantation embryo at E5.5, express pluripotent stem cell markers such as Oct4 and Nanog, and form cells of the three germ layers *in vitro* and *in vivo* (35-36). However, distinct differences in morphology, culture conditions, and gene expression profiles set EpiSCs apart from mESCs. Because EpiSCs exhibit upregulation of endodermal and ectodermal markers when compared to mESCs, EpiSCs are regarded as more lineage committed in developmental pathways.

Using lentivirus to deliver cre recombinase, we monitored infected *Dnmt1*^{2lox/2lox} EpiSCs for IAP protein reactivation. By 2 days post-infection, IAP protein was dramatically upregulated in Oct3/4 positive cells (Fig. 5). IAP signal remained high in the infected (gfp+) EpiSCs and their derivatives in early passages. However, demethylated EpiSCs do not survive passaging (our unpublished observations) and behave more like demethylated MEF cells (30).

Examine potential DNA methylation-independent IAP repression mechanism(s) in demethylated mESCs

Dnmt1^{-/-} mESCs appear to possess an alternative mechanism unique to embryonic stem cells to silence IAP elements in the absence of DNA methylation. Inhibition of histone deacetylases shift chromatin to a permissive state for transcription, relieving chromatin repression in mESCs(37). Histone deacetylase inhibitors significantly increased the number of IAP positive mESC colonies, as well as increasing the number of IAP positive cells per colony (Fig 6). However, IAP positive cells did not colocalize with strong Oct3/4 immunoreactivity (Fig 6A), thus cell differentiation, a known side effect of treatment with HDAC inhibitors, explains the increase in IAP immunoreactivity.

The 20S proteasome acts as a transcriptional silencer blocking nonspecific transcription initiation at intergenic and intragenic regions in mESCs(38). Since the majority of IAP LTR insertions are intergenic, we investigated whether this mechanism controls unwanted transcription of IAP elements. After treatment with the proteasome inhibitor MG132 for 8 hours, no colocalization of Oct3/4 and IAP immunostaining was seen in colonies examined (Fig 6C), nor was a dramatic rise of IAP mRNA present in treated *Dnmt1*^{-/-} mESCs (0.58 ± 0.17 fold change, p = 0.08). Since IAP reactivation was not seen in either wildtype or demethylated mESCs after MG132 treatment, proteasome-mediated degradation of intergenic gene transcription is probably not the alternative mechanism.

It has been postulated that Dicer protein mediated RNA interference or microRNA production could be a potential mechanism to block IAP expression. Minor demethylation of IAP elements are detected in *Dicer*^{-/-} mESCs (39). We therefore generated *Dnmt1*^{-/-}; *Dicer*^{-/-} double mutant ESCs using lentiviral cre recombinase, and examined by immunocytochemistry for the colocalization of IAP and Oct4. Individual subclones were genotyped via PCR for 2lox versus 1 lox detection at both loci, and quantitative RT-PCR verified the reduced expression of both *Dnmt1* and *Dicer* (Fig. 7). Although IAP protein was strongly expressed in spontaneously differentiating cells (Oct3/4 negative), we failed to detect the co-localization of strong IAP signal with Oct3/4 positive cells (Fig 7). It is of note that two clones showed a few cells (< 0.2% of the counted colonies) with weak juxtanuclear staining (Fig. 7). Our results argue against the possibility that Dicer-mediated RNA interference or microRNAs would be the alternative mechanism in repressing IAP expression in undifferentiated mESCs.

Discussion

Host cell defensive strategies have evolved to counteract the deleterious consequences of IAP element reactivation. The best-documented mechanism, DNA methylation of LTR promoters, can directly impede access of transcription factors or lead to an inactive form of chromatin at target loci (40). As our time course in MEF cells indicates, IAP protein expression is tightly correlated with genomic DNA methylation levels, making IAP protein reactivation a reliable

indicator of global changes in DNA methylation levels in individual cells. Previous tools for examining global DNA hypomethylation levels relied on evaluating DNA or RNA extracted from a population of cells. Although these techniques are sensitive, no evaluation could be made for global DNA methylation changes in individual cells within tissue. As shown in Figure 3, IAP immunohistochemistry allows for recognition of DNA demethylation at a cellular level in different tissue types. In cultured N2a mouse neuroblastoma cells, a robust reactivation of IAP protein is present. Similarly, in hypomethylated neural lineage cells, IAP protein can be used to trace the demethylation status at the individual cell level. Thus, IAP antibodies are valuable reagents to detect demethylated cells in the murine system.

Hypomethylated mESCs appear to possess an alternative mechanism for IAP silencing beyond the DNA methylation-mediated pathway. Interestingly, EpiSCs, which are also pluripotent yet differ from mESCs in both transcriptional networks and epigenetic modifications (35-36), show strong IAP protein reactivation after *Dnmt1* deletion. Thus, a methylation-independent repressional mechanism is unique to mESCs. Further analysis of transcriptional and epigenetic profiles may highlight this unique repressional mechanism in mESCs.

It can be potentially argued that DNA methylation directed by *de novo* methyltransferases in *Dnmt1*^{-/-} mESCs silence IAP elements. We evaluated IAP protein expression levels in *Dnmt1/Dnmt3a/Dnmt3b* deficient mESCs (TKO cells)(25). Under standard mESC culture conditions, the IAP positive TKO cell population was not Oct4 positive (Supplemental Figure 1). Since TKO cells have less than 2% of the normal methylation levels (25), we argue that mESCs possess an alternative mechanism in the absence of DNA methylation that mediates IAP gene silencing.

We have considered the involvement of both transcriptional and translational mechanisms controlling IAP expression in demethylated mESCs. It is possible that redundant repressive mechanisms are present in mESCs that include DNA methylation and histone modifications, yet HDAC inhibitors did not induce IAP expression in demethylated *Dnmt1*^{-/-} mESCs (Fig. 6). Furthermore, preliminary results showed that

deficiency of either PRC2 (*eed*^{-/-} mESCs) or PRC1 (*Bmi*^{-/-} brain tissues) alone did not relieve IAP protein repression (data not shown). To definitively ascertain PcG complex involvement, deficiency of both Polycomb complexes and DNA methylation in mESCs may be needed to trigger IAP protein expression.

Small RNA mediated silencing pathways have been reported to regulate retrotransposons. Presently, contradictory reports regarding Dicer involvement in IAP silencing appear in the literature. One group observed increased transcription from centromeric repeats, L1s, and IAPs (39); however, other groups state mammalian DICER and Eif2c2 (Ago2) have no roles in maintaining genomic methylation in mESCs, with direct evidence that the RISC complex does not repress IAP expression post-transcriptionally (41-42). Our double deletion model in mESCs reveals no large induction of IAP protein reactivation, arguing that Dicer-mediated transcriptional silencing is not strongly targeting IAP repression. While we observed weak IAP immunostaining in a few *Dnmt1*^{-/-}; *Dicer*^{-/-} cells, this could be due to the fact that Dicer mutation dramatically increases Oct3/4 levels in mESCs (39,41). The appearance of a few Oct3/4 immunopositive cells weakly co-stained for IAP could be explained by longer turnover of Oct3/4 protein, thus cells undergoing early stages of spontaneous differentiation would retain residual Oct3/4 protein.

While this manuscript was in preparation, two recent publications demonstrated that KAP1/Trim28 repressor protein coupled with histone lysine 9 methyltransferase KMT1E (ESET/SETDB1) is involved in repressed IAP gene transcription in mESCs (43-44). These studies revealed a novel role of repressive histone modifications as an alternative transcriptional repressive mechanism independent of DNA methylation. Interestingly, in the absence of all three Dnmts in mESCs, Matsui et al. (2010) reported KAP repressive complex remains associated with IAP retrotransposon elements(44). Furthermore, KAP1/Trim28 acts synergistically with DNA methylation to repress IAP transcription(43). However, none of the two groups have examined whether IAP proteins are present in KAP1^{-/-} mESCs. In our study, we found that IAP gene transcription is only moderately

increased when compared to differentiated *Dnmt1*^{-/-} cells. Furthermore, IAP protein is not detected in demethylated mESCs, consistent with an additional inhibitory mechanism that blocks IAP expression in undifferentiated mESCs.

Based on the findings of this current study, we conclude that IAP protein expression can be used to detect DNA hypomethylation at the cellular level in murine cells ranging from epiblast-derived stem cells to adult neurons. Both IAP transcription and protein translation can be detected upon DNA hypomethylation in lineage-committed cells. Yet in undifferentiated mESCs, there exists compensatory mechanism(s) to repress retrotransposon elements independent of DNA methylation. The need for an alternative mechanism further highlights the importance of maintaining genomic stability to prevent insertional mutations in fast replicating mESCs.

References:

1. Walsh, C. P., and Bestor, T. H. (1999) *Genes Dev* **13**, 26-34
2. Robertson, K. D., and Wolffe, A. P. (2000) *Nat Rev Genet* **1**, 11-19
3. Bestor, T. H. (2000) *Hum Mol Genet* **9**, 2395-2402
4. Watt, F., and Molloy, P. L. (1988) *Genes Dev* **2**, 1136-1143
5. Nan, X., Campoy, F. J., and Bird, A. (1997) *Cell* **88**, 471-481
6. Hendrich, B., and Bird, A. (1998) *Mol Cell Biol* **18**, 6538-6547
7. Ng, H. H., Zhang, Y., Hendrich, B., Johnson, C. A., Turner, B. M., Erdjument-Bromage, H., Tempst, P., Reinberg, D., and Bird, A. (1999) *Nat Genet* **23**, 58-61
8. Ng, H. H., Jeppesen, P., and Bird, A. (2000) *Mol Cell Biol* **20**, 1394-1406
9. Feng, J., Fouse, S., and Fan, G. (2007) *Pediatr Res* **61**, 58R-63R
10. Walsh, C. P., Chaillet, J. R., and Bestor, T. H. (1998) *Nat Genet* **20**, 116-117
11. Hutnick, L. K., Golshani, P., Namihira, M., Xue, Z., Matynia, A., Yang, X. W., Silva, A. J., Schweizer, F. E., and Fan, G. (2009) *Hum Mol Genet* **18**, 2875-2888
12. Heidmann, O., and Heidmann, T. (1991) *Cell* **64**, 159-170
13. Dupressoir, A., and Heidmann, T. (1996) *Mol Cell Biol* **16**, 4495-4503
14. Dewannieux, M., Dupressoir, A., Harper, F., Pierron, G., and Heidmann, T. (2004) *Nat Genet* **36**, 534-539
15. Whitelaw, E., and Martin, D. I. (2001) *Nat Genet* **27**, 361-365
16. Ukai, H., Ishii-Oba, H., Ukai-Tadenuma, M., Ogiu, T., and Tsuji, H. (2003) *Mol Carcinog* **37**, 110-119
17. Lee, J. S., Haruna, T., Ishimoto, A., Honjo, T., and Yanagawa, S. (1999) *J Virol* **73**, 5166-5171
18. Kuff, E. L., Wivel, N. A., and Lueders, K. K. (1968) *Cancer Res* **28**, 2137-2148
19. Gaudet, F., Rideout, W. M., 3rd, Meissner, A., Dausman, J., Leonhardt, H., and Jaenisch, R. (2004) *Mol Cell Biol* **24**, 1640-1648
20. Lees-Murdock, D. J., De Felici, M., and Walsh, C. P. (2003) *Genomics* **82**, 230-237
21. Kuff, E. L., Callahan, R., and Howk, R. S. (1980) *J Virol* **33**, 1211-1214
22. Mietz, J. A., Grossman, Z., Lueders, K. K., and Kuff, E. L. (1987) *J Virol* **61**, 3020-3029
23. Soriano, P. (1999) *Nat Genet* **21**, 70-71
24. Lei, H., Oh, S. P., Okano, M., Juttermann, R., Goss, K. A., Jaenisch, R., and Li, E. (1996) *Development* **122**, 3195-3205
25. Meissner, A., Gnirke, A., Bell, G. W., Ramsahoye, B., Lander, E. S., and Jaenisch, R. (2005) *Nucleic Acids Res* **33**, 5868-5877
26. Fan, G., Martinowich, K., Chin, M. H., He, F., Fouse, S. D., Hutnick, L., Hattori, D., Ge, W., Shen, Y., Wu, H., ten Hoeve, J., Shuai, K., and Sun, Y. E. (2005) *Development* **132**, 3345-3356
27. Livak, K. J., and Schmittgen, T. D. (2001) *Methods* **25**, 402-408
28. Shen, Y., Matsuno, Y., Fouse, S. D., Rao, N., Root, S., Xu, R., Pellegrini, M., Riggs, A. D., and Fan, G. (2008) *Proc Natl Acad Sci U S A* **105**, 4709-4714
29. Fan, G., Beard, C., Chen, R. Z., Csankovszki, G., Sun, Y., Siniaia, M., Biniszkiwicz, D., Bates, B., Lee, P. P., Kuhn, R., Trumpp, A., Poon, C., Wilson, C. B., and Jaenisch, R. (2001) *J Neurosci* **21**, 788-797

30. Jackson-Grusby, L., Beard, C., Possemato, R., Tudor, M., Fambrough, D., Csankovszki, G., Dausman, J., Lee, P., Wilson, C., Lander, E., and Jaenisch, R. (2001) *Nat Genet* **27**, 31-39
31. Connelly, M. A., Grady, R. C., Mushinski, J. F., and Marcu, K. B. (1994) *Proc Natl Acad Sci U S A* **91**, 1337-1341
32. Sugino, H., Toyama, T., Taguchi, Y., Esumi, S., Miyazaki, M., and Yagi, T. (2004) *Gene* **337**, 91-103
33. Binischkiewicz, D., Gribnau, J., Ramsahoye, B., Gaudet, F., Eggan, K., Humpherys, D., Mastrangelo, M. A., Jun, Z., Walter, J., and Jaenisch, R. (2002) *Mol Cell Biol* **22**, 2124-2135
34. Damelin, M., and Bestor, T. H. (2007) *Mol Cell Biol* **27**, 3891-3899
35. Tesar, P. J., Chenoweth, J. G., Brook, F. A., Davies, T. J., Evans, E. P., Mack, D. L., Gardner, R. L., and McKay, R. D. (2007) *Nature* **448**, 196-199
36. Brons, I. G., Smithers, L. E., Trotter, M. W., Rugg-Gunn, P., Sun, B., Chuva de Sousa Lopes, S. M., Howlett, S. K., Clarkson, A., Ahrlund-Richter, L., Pedersen, R. A., and Vallier, L. (2007) *Nature* **448**, 191-195
37. Schuettengruber, B., Chourrout, D., Vervoort, M., Leblanc, B., and Cavalli, G. (2007) *Cell* **128**, 735-745
38. Szutorisz, H., Georgiou, A., Tora, L., and Dillon, N. (2006) *Cell* **127**, 1375-1388
39. Kanellopoulou, C., Muljo, S. A., Kung, A. L., Ganesan, S., Drapkin, R., Jenuwein, T., Livingston, D. M., and Rajewsky, K. (2005) *Genes Dev* **19**, 489-501
40. Li, E. (2002) *Nat Rev Genet* **3**, 662-673
41. Murchison, E. P., Partridge, J. F., Tam, O. H., Cheloufi, S., and Hannon, G. J. (2005) *Proc Natl Acad Sci U S A* **102**, 12135-12140
42. Morita, S., Horii, T., Kimura, M., Goto, Y., Ochiya, T., and Hatada, I. (2007) *Genomics* **89**, 687-696
43. Rowe, H. M., Jakobsson, J., Mesnard, D., Rougemont, J., Reynard, S., Aktas, T., Maillard, P. V., Layard-Liesching, H., Verp, S., Marquis, J., Spitz, F., Constam, D. B., and Trono, D. (2010) *Nature* **463**, 237-240
44. Matsui, T., Leung, D., Miyashita, H., Maksakova, I. A., Miyachi, H., Kimura, H., Tachibana, M., Lorincz, M. C., and Shinkai, Y. (2010) *Nature*
45. Kuff, E. L., and Fewell, J. W. (1985) *Mol Cell Biol* **5**, 474-483

Footnotes

We thank Dr. Kira Lueders for the gifts of the p73 antibody and the MIA14 plasmid and Thuc Le for the editing of the manuscript. This work was supported by NIH RO1 grant NS051411 and NIH P01 GM081621(GF), California Institute of Regenerative Medicine RC1-0111 (GF), and NRSA 5F31NS051(LKH). GF is a Carol Moss Spivak Scholar in Neuroscience.

Figure Legends

Fig. 1.

IAP protein is only detected in lysates of E18.5 *Dnmt1*^{-/-} mutant brain.

A: Depiction of protein structural domains of the full length IAP clone MIA14. A deletion series of the gag peptide domain, which most closely corresponds to the p73 peptide used to generate the original IAP antibody (45), was cloned to create GST fusion peptides.

B: Immunoblotting revealing IAP expression in control (Con) and E18.5 *Nestin-cre; Dnmt1* conditional mutant brain lysate (Mut) of the original p73 serum before purification (anti-p73, left blot) and after column purification using the IAP 2-GST fusion peptide (anti-p73, middle blot). Our IAP2 polyclonal antibody also strongly recognizes the 73 kDa gag protein (anti-IAP2, right blot) from mutant brain lysate (Mut) (29).

Fig. 2.

IAP protein reactivation is tightly linked to the onset of DNA demethylation in MEFs.

A. *Dnmt1* 2lox/2lox MEFs were infected with MSCV-cre, and genomic demethylation was monitored using restriction enzyme digestion with methyl-sensitive HpaII followed by Southern blot analysis of IAP repetitive elements. Genomic demethylation appears four days after infection.

B. Immunoblotting shows that IAP protein expression appears 5 days post-infection with MSCV-cre, thus the IAP protein expression occurs after significant genome demethylation. The lane furthest to the right is a positive control for IAP proteins detected in the brain of E18.5 *Nestin-cre; Dnmt1* conditional knockouts (Brain E18.5 MUT) (29).

C. IAP immunocytochemistry (red) colocalizes with MSCV-cre-gfp infected cells (green) once the genome becomes significantly demethylated after DNMT1 deletion.

Fig 3.

Detection of IAP protein expression in demethylated somatic cells

A. Left panel: Immunoblotting using anti-IAP2 shows IAP protein in control and E18.5 *Nestin-cre; Dnmt1* conditional mutant brain lysates. Right panel: IAP immunoreactivity in E18.5 dorsal cortex of E18.5 *Nestin-cre; Dnmt1* mutant mice (29).

B. Left panel: Western blot analysis of IAP protein expression in control and *Emx1-cre; Dnmt1* cortical lysate from neonate P0 to 1.5 years old. Right panel: IAP immunoreactivity in the dorsal cortex of 6-months old *Emx1-cre; Dnmt1* mutant mice (11).

C: Immunocytochemistry for IAP protein in cultured N2a neuroblastoma cell lines. Western blot showing IAP expression in N2a cells, but not in other types of neuroblastoma cells including B104 and Hs 683 from ATCC.

Fig 4.

Expression of IAP protein is suppressed in *Dnmt1*^{-/-} mESCs and is only reactivated upon partial differentiation coupled with dramatic increases in IAP mRNAs.

A. IAP protein is not expressed in undifferentiated *Dnmt1*^{-/-} mESCs, even though *Dnmt1*^{-/-} cells possess less than 22% of normal genomic DNA methylation levels (24, 25). (scale bar= 25 microns).

B. Upon induction of differentiation of *Dnmt1*^{-/-} (c/c) mESCs in the absence of LIF treatment, IAP mRNA levels dramatically over the time course of six to nine days in culture. No induction of IAP expression was observed in wild-type control (J1) mESCs.

- C. IAP protein levels in the heterogeneous lysate of *Dnmt1*^{-/-} cells are also detected after 6 days of LIF withdrawal, reaching a detectable threshold by Western blot. The blot on the left is a longer exposure to show detectable IAP expression at Day 6 of LIF withdrawal.
- D. IAP immunocytochemistry shows that only Oct4 negative cells express IAP protein in *Dnmt1*^{-/-} ESCs. IAP expressing cells were detected in a small population (under 10 %) at Day 0-4 of differentiation, but reaching peak levels at Day 6-9 upon the induction of differentiation by LIF withdrawal. (Scale bar= 50 microns)
- E. IAP FISH analysis reveals that both wildtype (J1) and *Dnmt1*^{-/-} (c/c) undifferentiated colonies at Day 0 of LIF withdrawal do not express IAP mRNA. Upon LIF withdrawal to induce differentiation, partially differentiated *Dnmt1*^{-/-} cells migrating away from the colony express IAP RNA (arrowheads). *Dnmt1*^{-/-} cells with undifferentiated colony morphology (arrow) do not express IAP mRNA. (Scale bar= 25 microns)
- F. Northern blot analysis of IAP gag coding region reveals the dramatic induction of IAP mRNA as LIF is withdrawn from culture. Fold induction levels are assessed after normalization of 28s rRNA bands from wild type (J1) and *Dnmt1*^{-/-} (c/c) during the time course of differentiation.

Fig. 5.

Hypomethylated epiSCs rapidly induce IAP protein reactivation

- A. Photomicrographs of a representative colony 2 days after lentiviral cre-recombinase delivery to *Dnmt12lox/2lox* epiSCs. IAP immunoreactivity is present in Oct4 positive (blue) infected (GFP positive, green) epiSCs. (Scale bar= 25 microns)
- B. 4 days after lentiviral cre-recombinase delivery, colonies arising from infected EpiSCs show homogenous population of Oct4/IAP/GFP positive cells. (Scale bar= 25 microns)

Fig. 6.

Inhibition of histone deacetylases and proteasome activities does not lead to IAP protein expression in undifferentiated *Dnmt1*^{-/-} mESCs.

- A: HDAC inhibitor treatments of *Dnmt1*^{-/-} mESCs in the presence of LIF were performed to question whether blocking histone deacetylation, thus promoting the active chromatin conformation, in *Dnmt1*^{-/-} mESCs would lead to IAP protein expression in undifferentiated cells. Confocal images show that HDAC inhibitors do not reactivate IAP protein expression in *Dnmt1*^{-/-} mESCs, suggesting an alternative repressive mechanism is involved. (Scale bar= 25 microns)
- B: Cell counts show that HDAC inhibitors increase the number of IAP positive colonies, which correlates to the known differentiating effect of HDAC inhibitors in cell culture.
- C: After 8 hours of treatment with the proteasome inhibitor MG132, IAP protein was not visualized in Oct3/4 expressing *Dnmt1*^{-/-} mESCs (Confocal photomicrograph, scale bar= 25 microns).

Fig. 7.

Clonal analysis of IAP expression in *Dicer*^{-/-}; *Dnmt1*^{-/-} mESCs.

- A. IAP protein reactivation was counted in individual clones after genotyping was performed. The vast majority of IAP positive cells were Oct3/4 negative, thus indicating that only *Dicer*/*Dnmt1* double mutant mESCs express IAP after spontaneous differentiation. Of note, two clones had a few cells expressing weak levels of IAP protein in Oct3/4 positive cells. The

numbers on the X-axis denote the number of cells counted in three to six individual clones for the three genotypes (control: $Dnmt1^{2lox}$; $Dicer^{2lox}$. $Dnmt1^{-/-}$ mutant cells: $Dnmt1^{1lox}$; $Dicer^{2lox}$. $Dnmt1^{-/-}$; $Dicer^{-/-}$ double mutant ESCs: $Dnmt1^{1lox}$; $Dicer^{1lox}$).

B. Photomicrographs of clone 127, where differential levels of IAP are expressed. Strong IAP immunostaining is seen in differentiating (Oct3/4 negative) cells, whereas a weak perinuclear stain can be rarely seen in very few Oct3/4⁺ cells (arrow, bottom panel). (Scale bar= 25 microns)

Figure 1

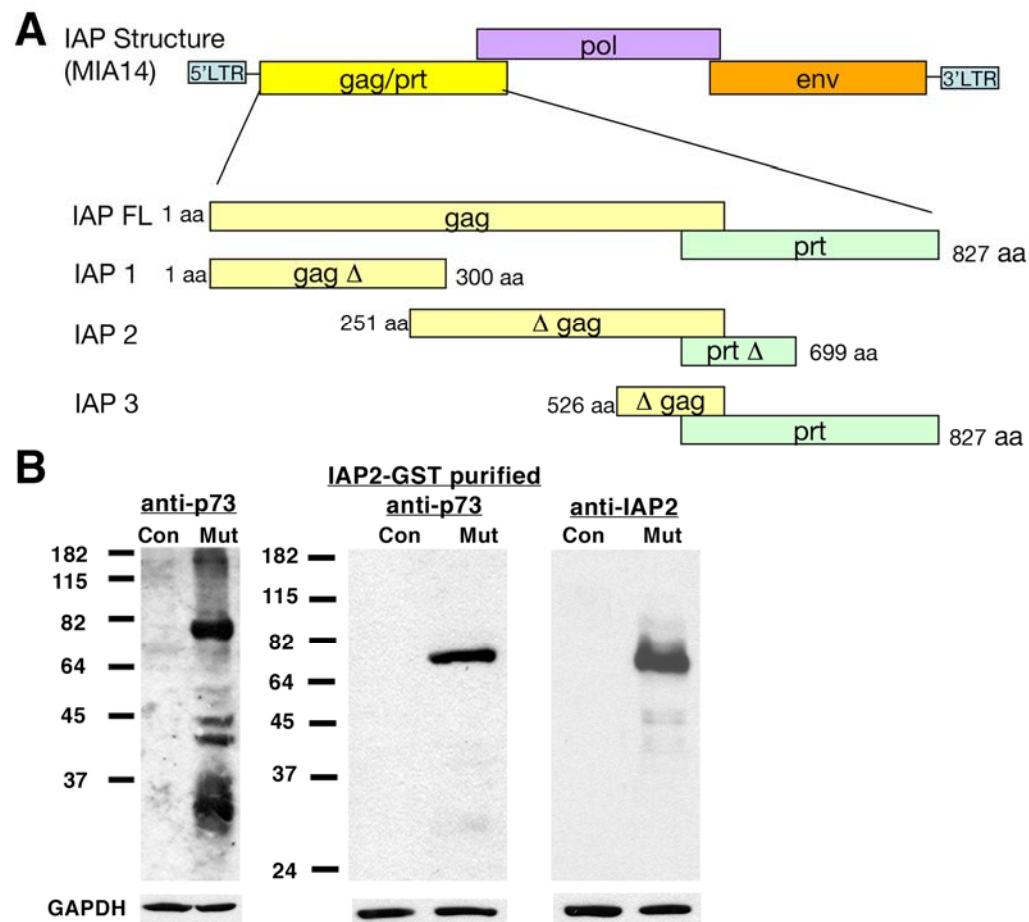


Figure 2

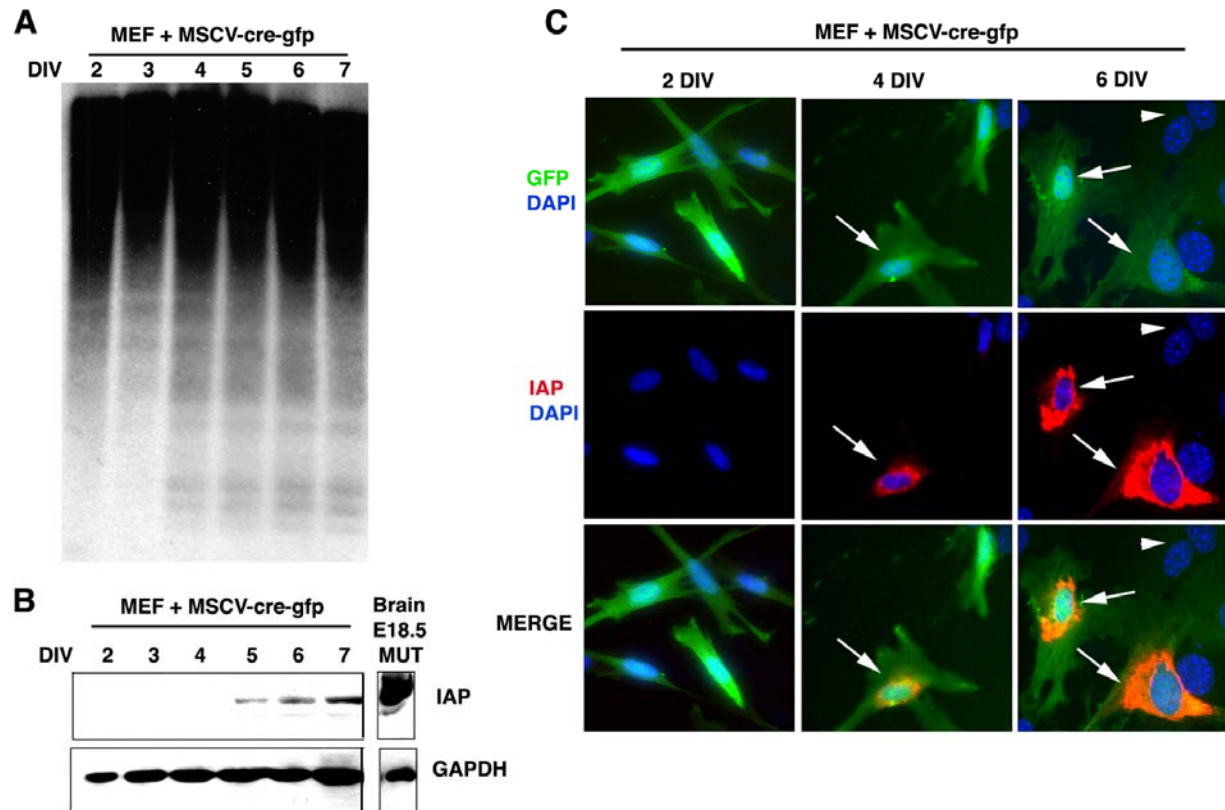


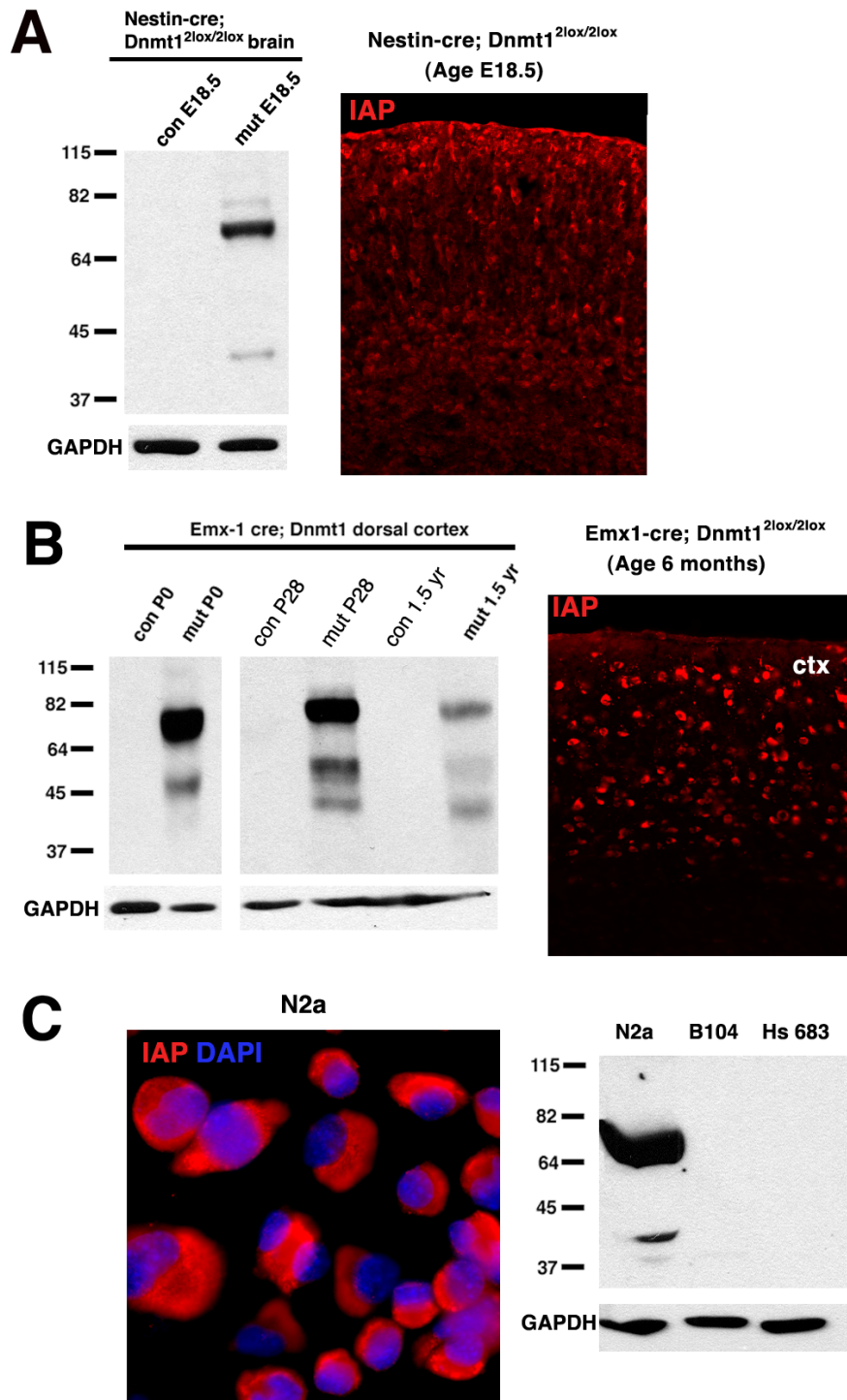
Figure 3



Figure 5

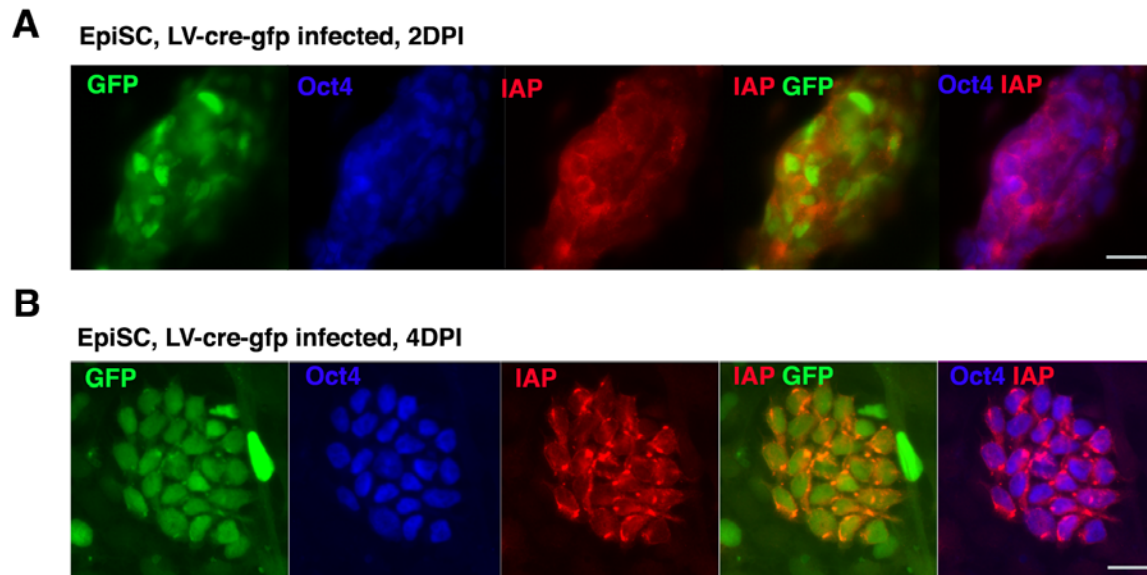


Figure 6

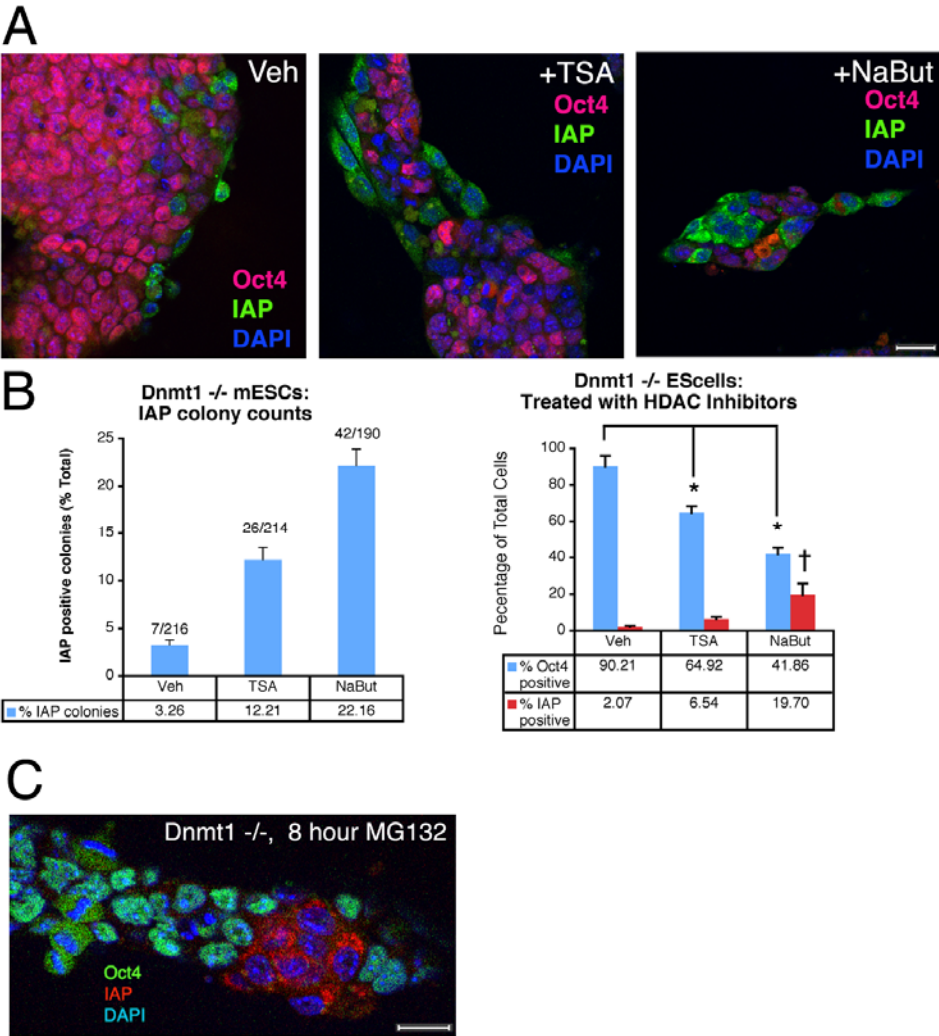
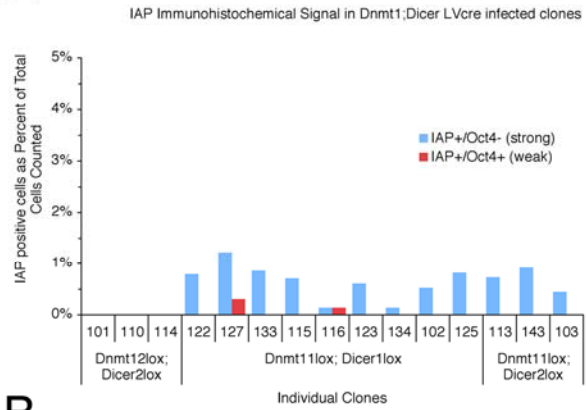
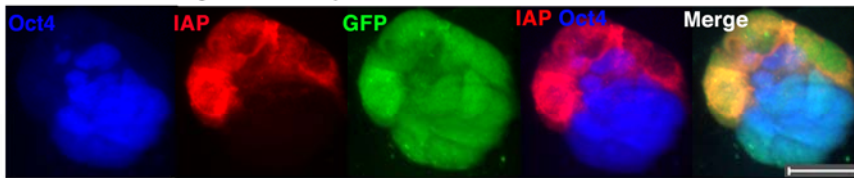


Figure 7**A****B**

127 clone: Strong IAP+ colony



127 clone: Weak IAP+ colony

